

Carbon fibre composites with ceramic and glass matrices

Part 2 *Continuous fibres*

R. A. J. SAMBELL, A. BRIGGS
Materials Development Division

D. C. PHILLIPS, D. H. BOWEN
Process Technology Division
AERE, Harwell, Didcot, Berks, UK

A description is given of the microstructure and mechanical properties of alumina, soda-lime glass, borosilicate glass and a lithia alumino-silicate glass-ceramic containing continuous, high modulus carbon fibres. Strengths up to 680 MNm^{-2} were obtained in glass samples containing 40 vol % of fibre whereas unreinforced glass had a strength of 100 MNm^{-2} . Works of fracture were typically 3 kJm^{-2} compared to 3 Jm^{-2} for unreinforced glass. The results are discussed in terms of volume fraction of fibre, fibre damage, matrix critical strain and stresses generated by a mismatch in the thermal expansion coefficients of the matrix and the fibres.

1. Introduction

It was shown in Part 1 [1] that the fracture energy of a ceramic can be increased by incorporating discontinuous brittle fibres to produce a composite material. Increased fracture energies were obtained with both random and aligned fibres, but increased strengths were only obtained when the fibres were aligned. Continuous fibres may in practice be aligned more easily than discontinuous fibres and higher volume fractions of reinforcement may be incorporated into the matrix. For these reasons continuous carbon fibre-ceramic matrix composites have been fabricated and this paper presents the results of a preliminary study of their properties. The ceramics studied were Pyrex glass, soda glass, a lithia alumino-silicate glass-ceramic and alumina.

2. Experimental

2.1. Fabrication

All the composites were produced by hot-pressing carbon fibres and ceramic powder in graphite dies in air, in a manner similar to that described in Part 1. No significant oxidation of the fibres occurred during this procedure, probably because of the formation of a carbon mon-

oxide atmosphere in the die. Composites were produced with fibre volume fractions between 20 and 60 vol %.

2.2. Testing

Bend (σ) and shear (τ) strengths were determined from three-point bend tests carried out on an Instron machine. Specimen cross-sections were $2.5 \times 1.0 \text{ mm}$ and the bending spans were 30 and 4mm respectively for bend and shear. The Instron cross-head speed was 0.1 mm min^{-1} and specimens were tested in the as-cut condition. Works of fracture were determined by measuring the energy absorbed when a bend specimen failed in a controlled manner [1].

2.3. Fibre volume fraction and matrix porosity

The volume fractions of fibre, open porosity and closed porosity quoted in Table II were calculated from the results of a series of burn-out and density measurements. The procedure used may be briefly summarized as follows. A specimen was first weighed in air (W_1). It was then placed in a vacuum chamber, the air was evacuated, the chamber was filled with water, and the saturated

TABLE I Typical property data for the different systems.

Material	Fibre content vol %	Bend strength MNm ⁻²	Shear strength MNm ⁻²	Work of fracture kJm ⁻²
Carbon fibre-Pyrex	40	680	64	3.4
Pyrex	0	100		0.003
Carbon fibre-glass-ceramic	36	680	46	3.0
Glass-ceramic	0	150		0.003
Carbon fibre-soda glass	45	570	48	4.3
Soda-glass	0	100		0.003

specimen was weighed in water (W_2). It was removed from the water, its surfaces were carefully dried without, as far as possible, removing water from the interior of the specimen, and it was re-weighed in air (W_3). The specimen was then placed in a furnace at 700°C in air until all the fibre was burned away, and finally weighed (W_4). It can be shown easily that the absolute volumes of the component phases are given by:

$$\text{Volume of fibres} = \frac{W_1 - W_4}{\rho_f}$$

$$\text{Volume of solid matrix} = \frac{W_4}{\rho_m}$$

$$\text{Volume of open porosity} = \frac{W_1 - W_3}{\rho_w}$$

$$\text{Volume of closed porosity} = \frac{(W_1 - W_2)}{\rho_w} - \frac{W_4}{\rho_m} - \frac{(W_1 - W_4)}{\rho_f}$$

where ρ_f , ρ_m and ρ_w are the densities of fibres, solid matrix and water respectively. The relative volume fractions may with care be measured to accuracies which are, for a 49 vol % fibre composite with 1 vol % of open and closed porosities:

$$\begin{aligned} V_f &= 49.0 \pm 0.4 \text{ vol \%} \\ V_m &= 49.0 \pm 0.4 \text{ vol \%} \\ V_{cp} &= 1.0 \pm 0.3 \text{ vol \%} \\ V_{op} &= 1.0 \pm 0.2 \text{ vol \%} \end{aligned}$$

3. Microstructure

The microstructures of polished sections of these materials were studied by optical microscopy in reflected light. Fig. 1 is a section parallel to the

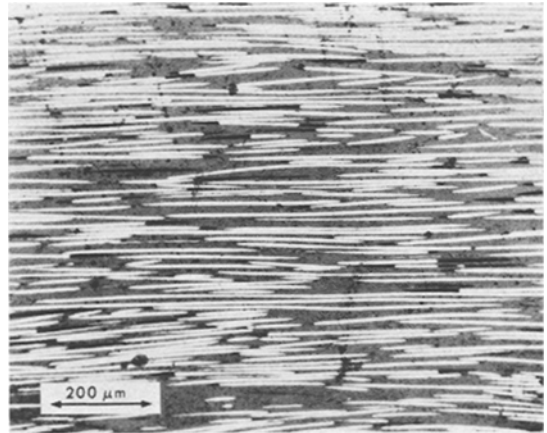


Figure 1 A section parallel to the fibres in carbon fibre reinforced Pyrex.

fibres of a carbon fibre reinforced Pyrex (CP) specimen. It illustrates the degree of alignment of the fibres in the composites and also shows that no cracking was observed in CP. Similarly the carbon fibre reinforced glass-ceramic (CGC) showed the same crack-free appearance. However, cracking did occur in carbon fibre reinforced soda glass (CS) and alumina (CA). In CS the cracking was localized and is best seen by observation in reflected light of a polished section perpendicular to the fibres as in Fig. 2. Interference fringes can be seen where the localized cracks are close to the polished surface. All the cracks are perpendicular to the fibre direction. In CA, cracking was very much more severe, regularly spaced cracks occurring in

TABLE II The effect of porosity on strength of CP.

Specimen	V_f	V_m	V_{op}	V_{cp}	σ	τ
A	37.8	55.4	6.1 ± 0.2	0.6 ± 0.3	450 ± 12	41 ± 1
B	38.8	59.4	1.1 ± 0.2	0.7 ± 0.3	607 ± 18	67 ± 2
C	37.8	61.1	0.8 ± 0.2	0.3 ± 0.3	510 ± 16	66 ± 1

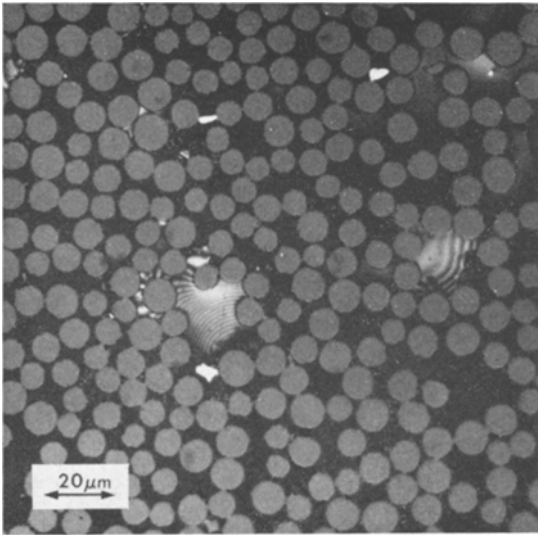


Figure 2 A section perpendicular to the fibres in carbon fibre reinforced soda glass.

planes perpendicular to the fibres and extending throughout the material.

4. Mechanical properties

Mean strengths and works of fracture of the various systems are shown in Table I. Comparisons of the different systems should be treated with caution because the fabrication conditions were not necessarily the optimum, and it will be shown that the mechanical properties were influenced by the choice of fabrication conditions.

The load-deflection behaviour in bending at room temperature of a typical specimen of CP

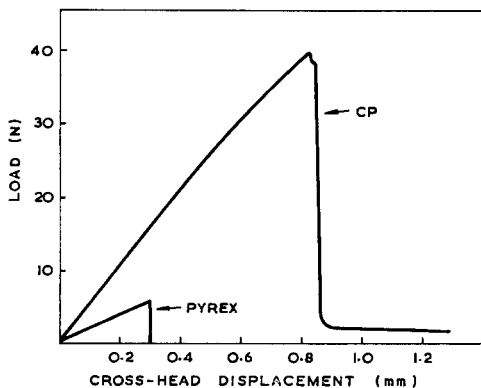


Figure 3 The load versus deflection behaviour of a strong sample of CP containing 40 vol % of fibre, and of Pyrex in bending at room temperature.

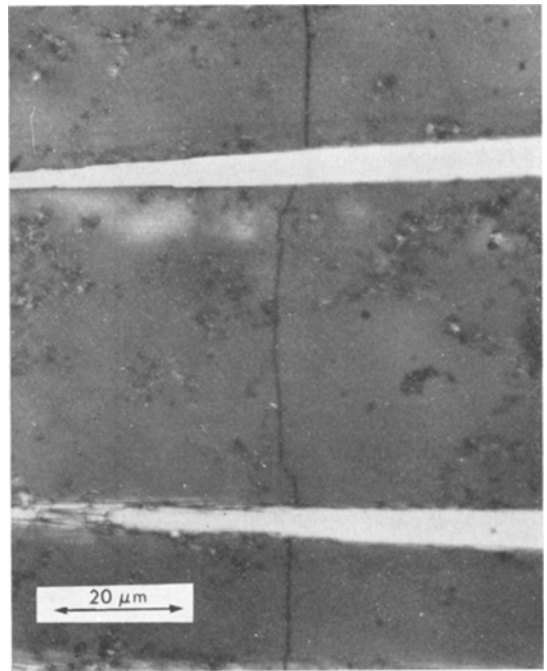


Figure 4 Microcracking in a CP matrix after stressing beyond the bendover stress.

from Table I is compared with that of unreinforced Pyrex in Fig. 3. This particular specimen contained 40 vol % of fibres and was manufactured under conditions which produced the highest strengths. The load-deflection curves of the CP specimens in Table I were linear up to a load corresponding to a mean maximum tensile stress of 340 MNm^{-2} after which there was a curvature associated with a decrease in modulus of the composite material. This curvature appeared to be due to the onset of matrix cracking in the tensile face. Fig. 4 is a photograph of fine microcracks which were produced by stressing a specimen beyond the bend in the load-deflection curve. These cracks did not exist in the material before loading, or on loading at stresses below the bendover, and they occurred only in the region of the specimen where the tensile stress was a maximum. Very similar behaviour was observed in the glass-ceramic and soda-glass matrix systems.

The elastic modulus of a 40 vol % CP specimen was measured by an ultrasonic pulse time of flight technique and a value of 169 GNm^{-2} was obtained.

The variation of bend strength and work of fracture with volume fraction of fibres in CP is

shown in Fig. 5. These specimens were produced under rather different hot-pressing conditions from the specimen described above and were of lower strength, but all samples were considerably stronger and tougher than the unreinforced matrix.

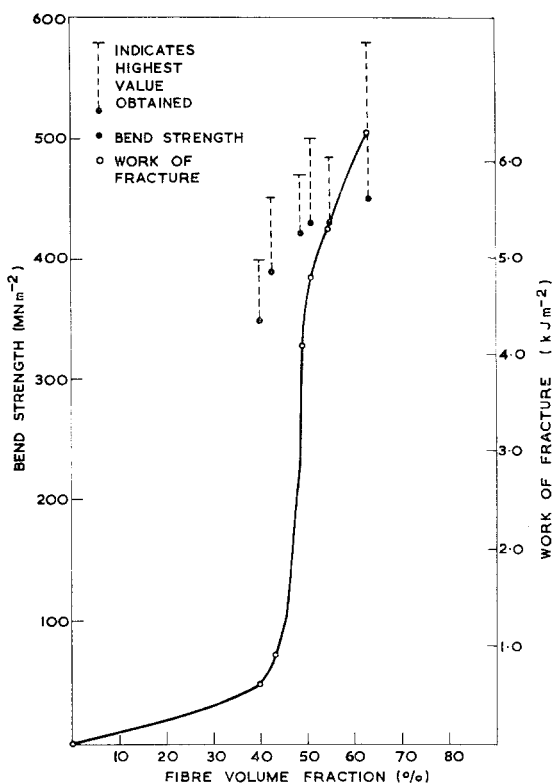


Figure 5 The variation of bend strength and work of fracture with fibre volume fraction in CP.

The strength of these carbon fibre composites was maintained at relatively high temperatures provided they were kept in an inert atmosphere. The strength of CP began to decrease at 500°C as the matrix softened, but the ceramic composites maintained their strengths to far higher temperatures. However, heating in air above the oxidizing temperature of the fibres degraded the mechanical properties of the composites.

Altering the fabrication conditions caused changes in the mechanical properties. These variations appeared to depend primarily on porosity in the matrix and damage to the fibres. Table II shows typical results obtained by varying only the maximum temperatures and pressures employed during hot-pressing CP. Specimen A was produced at a lower temperature than

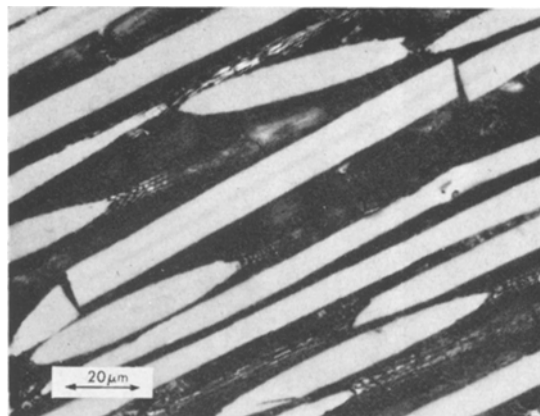


Figure 6 Gross fibre damage in a weak sample of CP.

B and C. Specimens B and C were produced at the same temperature but C was compacted at the higher pressure. The bend strengths and shear strengths quoted are each the means of six specimens and the errors quoted are the standard errors.

Fibres were studied in composites of similar porosities but different strengths and it was observed that there was more damage to fibres in the weaker materials. For example, Fig. 6 shows a polished section parallel to the fibres in one of the weaker samples of CP, illustrating the gross fibre damage which could occur. There was far less indication of broken fibres in stronger specimens. This was confirmed by dissolving in HF the matrices of similar high and low strength systems. Fibres from the higher strength specimens tended to be longer.

5. Discussion

5.1. Fracture strength

For unidirectional, continuous fibre composites in which stress is transferred from the matrix to the fibres by purely elastic deformation the ultimate tensile strength parallel to the fibres (σ_c) can frequently be represented by a simple mixtures law (see e.g. [2])

$$\sigma_c = (\sigma_f)_u V_f + \sigma_m V_m \quad (1)$$

where $(\sigma_f)_u$ is the UTS of the fibres, σ_m is the stress in the matrix when the stress in the fibres is $(\sigma_f)_u$, and V_f and V_m are the volume fractions of fibre and matrix respectively.

A fundamental difference between carbon fibre reinforced glasses and ceramics and carbon fibre reinforced resins and metals is that, in the case of resin and metal composites the critical

strain of the matrix is in general greater than that of the fibres whereas, in the case of the glass and ceramic composites, the critical strain of the matrix is less than that of the fibres. Thus, on deforming the resin and metal composites, the fibres are likely to fail before the matrix fractures, while for the glass and ceramic composites, provided the longitudinal strains in the matrix (ϵ_m) and the fibres (ϵ_f) are equal, it is to be expected that the matrix will fail before the fibres reach their fracture stress. In this case,

$$\epsilon_m = \epsilon_f = \frac{\sigma_m}{E_m} = \frac{\sigma_f}{E_f} \quad (2)$$

and assuming that the composite fails when the critical strain of the matrix is exceeded, the expected fracture stress is given by substituting Equation 2 in Equation 1.

$$\sigma_c = (\sigma_m)_u \left\{ 1 + V_f \left(\frac{E_f}{E_m} - 1 \right) \right\} \quad (3)$$

Equations 1 and 3 can be regarded as giving upper and lower estimates of the fracture stress depending on whether fracture of the fibres or of the matrix is the primary cause of failure. The modulus of the fibres used in this work was 390 GNm⁻² and the fibre strengths measured by whole tow tests on specimens with a gauge length of about 100 mm were typically about 1950 MNm⁻². The strength of Pyrex is about 100 MNm⁻² and the modulus 60 GNm⁻². If these figures are employed in Equations 1 and 3 the calculated fracture stresses for a 40 vol % composite are respectively 320 and 840 MNm⁻². These values may be compared with the experimental values for CP produced under the best known fabrication conditions. The mean UTS of 40 vol % material was 680 MNm⁻² and the bendover stress at which matrix cracking occurred was 340 MNm⁻². Thus the UTS corresponds more closely to that calculated from Equation 1 than to that from Equation 3, and the bend in the load-deflection curve occurs at a stress which corresponds to that calculated from Equation 3.

The theoretical strength of 840 MNm⁻² calculated from Equation 1 is significantly higher than the observed strength of 680 MNm⁻². However, because of the occurrence of matrix cracking at stresses lower than the UTS a more correct expression than $(\sigma_f)_u V_f + \sigma_m V_m$ would be simply $(\sigma_f)_u V_f$. This reduces the theoretical strength to 780 MNm⁻². It is not possible to compare the experimental strength of a com-

posite with a good theoretical prediction based on fibre and matrix properties because no accurate theory of composite strength yet exists. The mixtures law is at best an approximation and does not take into account the statistical distribution of fibre strengths and the interaction between fibre failures. Furthermore there is difficulty in knowing what value of fibre strength should be used. Different fibre testing techniques, such as whole tow and single fibre, give different mean strength values, while any one method reveals variations of mean strength along a tow. In addition the measured strengths of carbon fibres vary with gauge length [3] and it might be more appropriate to use, in the mixture law, a strength obtained from a gauge length which is of the order of the transfer length of the system. This, in CP is $\sim 200 \mu\text{m}$ [1].

5.2. Young's modulus

The Young's modulus of a composite (E_c) in the direction of the fibres is theoretically predicted by an expression analogous to Equation 1,

$$E_c = E_f V_f + E_m V_m \quad (4)$$

The value calculated for 40 vol % of carbon fibres in Pyrex glass is 196 GNm⁻² as compared with the measured value of 168 GNm⁻².

5.3. Thermal expansion mismatch

The results of this work differ from that described in Part 1 primarily in the behaviour of the CS system. For both discontinuous and continuous fibres, CP and CGC were uncracked, and CA was extensively cracked. However, CS was only slightly cracked when the fibres were continuous and aligned, but appeared very much more cracked when random and discontinuous. Cracking in the continuous fibre composites occurred perpendicularly to the fibres, indicating that it was a result of the mismatch between the fibre axial expansion coefficient and that of the matrix. It might be expected, therefore, that a continuous aligned composite containing a high volume fraction of fibre would exhibit more cracking than a low volume fraction, random fibre composite. Two reasons can be suggested as to why, in CS, the opposite is observed. (i) The expansion mismatch of discontinuous fibres would tend to lead to large stresses near the fibre ends. In a continuous fibre composite there would be relatively few fibre ends and thus a smaller contribution to matrix failure due to these stresses. (ii) The discontinuous CS system

contained a smaller volume fraction of fibres and thus might have tended to exhibit more cracking because there were fewer crack stoppers.

Complicated expressions exist for the calculation of the thermal expansion mismatch stresses in a continuous aligned fibre composite [4] but a simple, approximate formula may be derived for the axial stress (σ_a) in a matrix when the radial stresses are low. Thus:

$$\sigma_a = (\alpha_m - \alpha_f) \Delta T \frac{E_f V_f}{V_f \left(\frac{E_f}{E_m} - 1 \right) + 1} \quad (5)$$

Table III shows the calculated axial mismatch for 50 vol % of fibres. In the case of CA, σ_a is very much greater than the strength of the matrix, while for CP and CGC it is lower, in accordance with the observed cracking of CA and the crack-free appearances of CP and CGC. In the case of CS, $\sigma_a \approx 220 \text{ MNm}^{-2}$ as opposed to the value of 100 MNm^{-2} for the strength of as-cut soda glass. The fact that $\sigma_a > 100 \text{ MNm}^{-2}$ and that cracks are observed to be localized in CS, suggest that the presence of fibres inhibits the growth of cracks and strengthens the matrix.

6. Conclusions

- (1) Carbon fibre reinforced ceramics have been produced by hot-pressing. Their mechanical properties were influenced by matrix porosity and fibre damage.
- (2) Severe matrix cracking occurred in reinforced alumina due to thermal expansion mismatch,

localized cracking occurred in reinforced soda glass, reinforced Pyrex and glass-ceramic were crack-free.

- (3) The strengths of the reinforced glasses and glass-ceramic approached the predictions of the mixtures law.
- (4) Matrix cracking occurred at stresses well below the UTS of the composite.
- (5) Carbon fibre reinforced ceramics have high works of fracture compared with unreinforced ceramics.
- (6) Carbon fibre reinforced ceramics maintain their strengths in an inert atmosphere at high temperatures but are degraded by oxidation of the fibres.

Acknowledgements

The authors are grateful to their colleagues who have assisted, in various ways, in this work, and in particular to Mr J. Matthews and Mr P. Wightman for experimental assistance in the early stages of Part I and to Mr N. J. Mattingley throughout.

References

1. R. A. J. SAMBELL, D. H. BOWEN, and D. C. PHILLIPS, *J. Mater. Sci.* **7** (1972) 663.
2. A. KELLY and G. J. DAVIES, *Metall. Revs.* **10** (1965) 1.
3. R. MORETON, *Fibre Sci. and Tech.* **1** (1969) 273.
4. D. M. KARPINOS and L. I. TUCHINSKII, *Sov. Powder Metal. and Met. Ceram. English Transl.* **9** (1968) 735.

Received 23 December 1971 and accepted 3 January 1972.

TABLE III Axial thermal mismatch stresses in the matrices for 50 vol % of fibres.

Ceramic	α ($^{\circ}\text{C}^{-1}$)	ΔT ($^{\circ}\text{C}$)	E_m GNm^{-2}	σ_a MNm^{-2}	σ_m MNm^{-2}
Alumina	8×10^{-6}	1400	230	1570	300
Soda glass	9×10^{-6}	480	60	220	100
Pyrex	3.3×10^{-6}	520	60	88	100
Glass-ceramic	1.5×10^{-6}	1000	100	117	150